

# Structural Characterisation of End-of-Life Cement–Asbestos Materials from Lithuania

Robert Kusiorowski <sup>1,\*</sup> , Anna Gerle <sup>1</sup>, Magdalena Kujawa <sup>1</sup>, Valentin Antonovič <sup>2</sup> and Renata Boris <sup>2</sup>

<sup>1</sup> Lukaszewicz Research Network—Institute of Ceramics and Building Materials, Cementowa 8, 31-983 Cracow, Poland; anna.gerle@icimb.lukasiewicz.gov.pl (A.G.); magdalena.kujawa@icimb.lukasiewicz.gov.pl (M.K.)

<sup>2</sup> Laboratory of Composite Materials, Institute of Building Materials, Faculty of Civil Engineering, Vilnius Gediminas Technical University, Linkmenu St. 28, 08217 Vilnius, Lithuania; valentin.antonovic@vilniustech.lt (V.A.); renata.boris@vilniustech.lt (R.B.)

\* Correspondence: robert.kusiorowski@icimb.lukasiewicz.gov.pl or robert.kusiorowski@interia.pl; Tel.: +48-32-270-1939

**Abstract:** Asbestos is a widely used name for natural silicate minerals with fibrous properties. Asbestos minerals were one of the most popular and cheapest raw materials used in the construction industry in the past when they were used in the form of cement–asbestos composite material. Nowadays, we know that asbestos possesses carcinogenic properties. Due to this fact, asbestos was banned in many countries including Lithuania. All asbestos-containing materials are considered waste and stored in special landfills, which causes significant environmental pollution. One of the methods proposed to solve the asbestos problem may be thermal treatment. In the present study, asbestos-containing wastes in the form of cement–asbestos materials were examined. These asbestos-containing materials were characterised via chemical analysis (XRF) connected with mineralogical phase analysis with powder X-ray diffraction (XRD) as well as scanning electron microscopy (SEM). The thermal decomposition of samples was studied via differential thermal analysis (DTA) and thermogravimetric measurements with evolved gas analysis (TG–EGA). It was found that thermal treatment is a possible way to destroy asbestos contained in cement–asbestos wastes and convert it into new mineral phases. The work also compared the obtained characteristics of asbestos waste with the characteristics of waste produced in other countries.

**Keywords:** asbestos wastes; Lithuania; thermal treatment; decomposition



**Citation:** Kusiorowski, R.; Gerle, A.; Kujawa, M.; Antonovič, V.; Boris, R. Structural Characterisation of End-of-Life Cement–Asbestos Materials from Lithuania. *Fibers* **2024**, *12*, 37. <https://doi.org/10.3390/fib12040037>

Academic Editor: Koon-Yang Lee

Received: 17 January 2024

Revised: 5 April 2024

Accepted: 10 April 2024

Published: 15 April 2024



**Copyright:** © 2024 by the authors. Licensee MDPI, Basel, Switzerland. This article is an open access article distributed under the terms and conditions of the Creative Commons Attribution (CC BY) license (<https://creativecommons.org/licenses/by/4.0/>).

## 1. Introduction

Asbestos is a group of natural, hydrated silicate minerals (including chrysotile, amosite, and crocidolite), characterised by a fibrous form. It has unique physical and chemical properties, including high elasticity and mechanical strength, as well as resistance to temperature and chemicals (acids and alkalis). These unusual properties, combined with their widespread occurrence, contributed to the great industrial importance of asbestos in the past. It was used mainly in construction, primarily for the production of roofs, pipes, facade fragments and other construction elements [1–5]. Asbestos is a material that is difficult to naturally biodegrade [6]. Moreover, it has been proven that asbestos is a carcinogenic and mutagenic substance [7–9]. It occurs in the air in the dangerous form of microscopic fibres contributing to long-term diseases and latent development [10,11].

Therefore, despite its initial advantages, over the years, asbestos and all products made from it have become an undesirable material, considered in some countries to be hazardous waste. Today, only about 60–70 countries in the world [12–14] prohibit its use, and it is still a widely used building material in countries such as China, Russia, Brazil, India and Indonesia [14,15]. These countries are responsible for 85% of the total asbestos

consumption in the world. Over recent years, asbestos mining and production have been at the level of approximately 1.3 million tonnes per year [15].

The ban on the use of asbestos applies mainly in developed countries. Importantly, in all European Union countries, a complete ban on the use of asbestos was introduced on 1 January 2005 [16]. Asbestos and all products based on it are completely banned and not allowed for production or trade. In Poland, actions regarding the asbestos problem already took place earlier. Following the provisions of the relevant act [17] in 1998, among others, the production of asbestos–cement boards and trade in asbestos and products containing asbestos were prohibited. Moreover, in May 2002, the Council of Ministers adopted a long-term, 30-year national “Program for the removal of asbestos and asbestos-containing products used in the territory of Poland” [18].

The asbestos problem is particularly acute in the former Eastern Bloc and post-Soviet countries. Lithuania may be an example next to Poland. According to the literature data, over the years, 0.7 million tons of asbestos were imported into Lithuania, mainly for the production of cement–asbestos products [19–22]. This was due to rapid development after the end of World War II and the need to recover the damage, especially in the field of residential construction and industrial factories. Until 1990, asbestos was used in Lithuania in very large quantities, primarily in industrial facilities, where the main raw material was chrysotile from Russia and Kazakhstan [19–22]. In 1998, the document “The rules on work with asbestos” was created in Lithuania, and its assumptions were based on the European Council directives 80/1107/EEC [23], 83/477/EEC [24] and 91/382/EEC [25]. In 2004, the import and use of asbestos were completely banned [26].

Comparing the problem of asbestos waste in the two countries mentioned above, it is particularly large in the case of Lithuania, and it can be shown that it is much larger than that in Poland [27]. Taking into account the estimated data on the amount of asbestos imported into individual countries over the years, as well as the number of inhabitants and the area of the country, we can attempt to calculate and compare asbestos burden indicators (Table 1).

**Table 1.** The burden of asbestos on the country.

	Poland	Lithuania
Estimated amount of asbestos wastes; mln tonnes	15.5	4.5
The number of residents; mln	37.7	2.8
Area of the country; km <sup>2</sup>	313,000	63,500
Asbestos wastes per person; tons/person	0.4	1.6
Asbestos wastes per area; tons/km <sup>2</sup>	49.5	71.0

As we can see, even though Lithuania is about 5 times smaller than Poland and is almost 10 times less populated, the amount of accumulated asbestos waste is drastically higher. Taking into account the amount of waste per person in Lithuania, the calculated rate is four times higher than in the case of Polish citizens. According to estimates, there is approximately 1600 kg of asbestos waste per average Lithuanian resident. The amount of asbestos waste per unit area is also significantly higher.

Given the significant amount of accumulated waste containing asbestos, solving the asbestos problem is not an easy matter. Although the recommended method of dealing with asbestos waste is to deposit it in landfills [18], this is ultimately not an environmentally friendly solution. Although it solves the problem in the short term, it poses a huge burden on the environment and will be problematic for future generations. Also important is the presence of illegal landfills, which also contribute to the contamination of the natural environment [28].

According to EU authorities [29,30], the creation of asbestos waste dumps is only a temporary solution to the problem, which is thus left to future generations, because asbestos fibres hardly deteriorate over time. Therefore, knowledge about systems for the destruction of asbestos waste should be disseminated and scientific research and innovation

should be supported to apply technologies for the processing and disposal of asbestos-containing waste, to enable their safe recycling and to reuse and reduce their disposal products in landfills.

Asbestos disposal and recycling methods have been the subject of many studies. Several dozen technologies for the utilisation of this material have been patented around the world. Most of the proposed techniques concern the destruction of the harmful structure of asbestos fibres and transformation of them into recyclable material. In terms of the factor initiating asbestos structure destruction, the methods of utilising asbestos and cement–asbestos products found in the literature and thoroughly described [31–33] can be generally divided into four main areas, i.e., chemical, biological, mechanochemical and thermal methods. Each method has its advantages and disadvantages [27,33]. One of the interesting solutions for the degradation of asbestos waste that has appeared in recent years is the carbonisation method, which involves exposing the prepared asbestos material to CO<sub>2</sub> gas [34,35]. This work is promising and particularly useful when searching for methods of capturing and sequestering CO<sub>2</sub> from the atmosphere to create stable carbonate phases [36,37].

The thermal method seems to be the most prospective [38,39], due to the lack of harmful post-process reagents and the relatively short process time [40]. Thermal methods have a lower environmental impact than do other proposed asbestos recycling processes. Heat treatment is used to transform asbestos into an inert material within the temperature range at which the fibres become unstable. Due to the applied temperature and the conditions of the thermal treatment process, the destruction of the hazardous form of asbestos may occur in different ways, leading to thermal decomposition related to asbestos mineral dehydroxylation and further full crystal–chemical transformation or its melting in vitrification processes. Asbestos can be thermally utilised by using various sources of heat, e.g., conventional, hydrothermal, microwave and plasma. Although thermal methods may be instinctively considered energy-intensive and emission-intensive, the assumptions of the Green Deal may contribute to the competitiveness of thermal methods in the future, e.g., by switching to emission-free technologies, e.g., hydrogenous technologies, or via the use of renewable energy sources. Because asbestos minerals belong to the group of hydrated silicates, at a sufficiently high temperature, they undergo a dehydroxylation reaction and are consequently transformed into new mineral phases with different crystal structures [41–45]. Similar behaviour should be expected in the case of asbestos waste, including cement–asbestos waste [46–52].

The aim of this work was therefore to structurally characterise several Lithuanian end-of-life asbestos wastes in terms of their chemical and phase composition and to determine the course of thermal decomposition in the context of possible thermal treatment. For the first time, this characterisation was conducted for waste from Lithuania and compared with that of Polish waste. This is crucial because issues regarding the necessity of testing asbestos waste from Eastern Europe are relatively rare in the scientific literature.

## 2. Materials and Methods

Three end-of-life asbestos-containing materials coming from Lithuania were tested. All materials used in the present study were in an “as received” state, without any further purification. All tested samples were corrugated cement–asbestos boards (Figure 1a), but they varied in terms of the place of collection and the time of use and operation. Sample 1 (TR) came from the vicinity of Trakai, which in fragmented form was used as the hardening agent of local grounds on private property. This sample had been in contact with the external environment for several years. Samples 2 and 3 (V2 and V5, respectively) were dismantled cement–asbestos boards from the same private estate near Vilnius but differed in the time of use on the roof. The V2 sample was approximately 20 years old from purchase and installation on the roof, while the V5 sample was approximately 50 years old.



**Figure 1.** The primary appearance of tested samples and optical microscope view of the widths (a); the view of pieces of samples after thermal treatment at 1100 °C (b).

The samples considered differed significantly visually. In the case of the V5 sample, significant leaching out of the matrix components could be observed, and the material itself no longer showed high mechanical strength. Under slight pressure, pieces of the cement–asbestos board could be easily broken off. Moreover, in the case of this sample, delamination of the material could be observed. The remaining two samples looked similar to each other, although in the case of the TR sample, some rusty discolouration could be observed on the surface and inside the board. The width of the cement–asbestos boards, which was established, according to optical microscopy analysis, was ~5–7 mm. A visualisation of the pieces of samples after thermal treatment at 1100 °C is presented (Figure 1b).

These raw cement–asbestos materials were studied using different techniques like X-ray fluorescence (XRF), differential thermal analysis (DTA), thermogravimetric analysis (TG/DTG) with evolved gas analysis (EGA), X-ray powder diffraction (XRD), optical microscopy (OM) and scanning electron microscopy (SEM). Additionally, all cement–asbestos samples were isothermally fired in porcelain crucibles at 1100 °C for 4 h in an electric muffle laboratory furnace (model LT 9/14, Nabertherm, Lilienthal, Germany), and subsequent studies were performed on the obtained materials (OM, XRD, SEM). This temperature was selected based on that in the literature [52].

Simultaneous differential thermal analysis (DTA), thermogravimetric analysis (TG), differential thermogravimetric analysis (DTG) and the measurement of gases that evolved from the samples (EGA) were carried out using a simultaneous STA 409 PC Luxx thermal analyser coupled with a QMS 403 C Aeolos quadrupole mass spectrometer (Netzsch, Selb, Germany). All experiments were performed to up to 1450 °C in an airflow of 30 mL/min at a heating rate of 20 °C min<sup>-1</sup> using an open alumina crucible with about 100 mg of sample.

For the phase analysis of the raw and calcined cement–asbestos, X-ray powder diffraction (PANalytical X’pert Pro diffractometer, with CuK $\alpha$  radiation, Ni filter, 40 kV, 30 mA, X’Celerator detector, Malvern PANalytical, Almelo, The Netherlands) was used. The phase composition was determined through the diffraction peaks connecting with the identified phases using HighScore Plus software (version 5.1; Malvern PANalytical, Almelo, The Netherlands) and the ICDD PDF-4+ database.

The chemical composition analysis using X-ray fluorescence (XRF) was performed in accordance with EN ISO 12677:2011 [53]. Once ignited to a constant mass, the sample was melted with a commercially available mixture of lithium tetraborate, lithium metaborate and lithium bromide (66.67%, 32.83%, and 0.5%), characterised by a flux purity adequate for XRF (from Spex, Long Island City, NY, USA). The sample-to-flux weight ratio was 1:9. The samples to be analysed were prepared by melting their mineralogical and grain structure until destroyed. The samples prepared in this way were measured using the PANalytical MagiX PW2424 spectrometer from Malvern PANalytical, Almelo, The Netherlands, calibrated using a series of certified reference materials: JRRM 121-135, JRRM 201-210 and JRRM 301-310 (Technical Association of Refractories, Tokyo, Japan). The chemical analysis was supplemented by including the content of volatile components. They were measured via calcination at 1025 °C to a constant weight in an electric laboratory furnace and expressed as a value of loss on ignition (L.O.I.).

Microstructure analysis was performed using a Mira 3 electron microscope (Tescan, Brno, Czech Republic) equipped with an energy-dispersive spectrometer (EDS) system with AZtec Automated ver. 3.1 software (Oxford Instruments, Abingdon, UK). The analysis was performed at an accelerating voltage of 15 kV in the backscattered electron mode (BSE) or secondary electron mode (SE) for image formation. The measurements were carried out on the samples covered by a conductive layer of chromium by using a Quorum Q150R ES device (Quorum Technologies, Laughton, UK). Initial widths of samples were measured using a stereo microscope (Zeiss, Stemi 305, Munich, Germany), equipped with a 5.0-megapixel digital camera (AxioCam ERc 5s, Munich, Germany).

### 3. Results

#### 3.1. X-ray Fluorescence Characterisation

The chemical compositions of tested Lithuanian raw cement–asbestos wastes are presented in Table 2. The chemical compositions are dominated by SiO<sub>2</sub> (ca 33 wt%) and CaO (ca 25–30 wt%). The very high loss on ignition value is also noteworthy; it changed from ~20 to 25 wt%. This was most likely related to the strong carbonation of the samples, especially in the case of the TR and V5 samples, which could have been operated in external conditions for a longer time. Besides these components, there are also accompanying ingredients like MgO (ca 6 wt%), iron compounds (converted into Fe<sub>2</sub>O<sub>3</sub>, 3–5 wt%) and Al<sub>2</sub>O<sub>3</sub> (ca 4 wt%) that are presented. The chemical composition is supplemented with ingredients present in amounts below 1% (TiO<sub>2</sub>, Na<sub>2</sub>O, K<sub>2</sub>O and SO<sub>3</sub>). If uncertainties are taken into account, the differences in MgO are negligible. However, the TR sample had a slightly higher Fe<sub>2</sub>O<sub>3</sub> content, which was most likely due to the presence of corrosion products of metal fastening elements or secondary contamination during “ageing” on the ground, for example.

**Table 2.** Results of raw cement–asbestos chemical analysis (values in wt%).

Sample	TR	V2	V5
SiO <sub>2</sub>	33.1 ± 1.5	33.4 ± 1.5	32.1 ± 1.4
TiO <sub>2</sub>	0.2 ± 0.1	0.2 ± 0.1	0.2 ± 0.1
Al <sub>2</sub> O <sub>3</sub>	3.6 ± 0.3	3.8 ± 0.3	3.9 ± 0.3
Fe <sub>2</sub> O <sub>3</sub>	5.2 ± 0.2	3.4 ± 0.1	3.1 ± 0.1
MgO	6.5 ± 0.5	5.7 ± 0.4	5.6 ± 0.4
CaO	25.5 ± 1.2	33.5 ± 1.6	29.2 ± 1.4
Na <sub>2</sub> O	0.1 ± 0.1	0.1 ± 0.1	0.1 ± 0.1
K <sub>2</sub> O	0.6 ± 0.1	0.3 ± 0.1	0.3 ± 0.1
SO <sub>3</sub>	0.3 ± 0.1	0.4 ± 0.1	0.6 ± 0.2
LOI	24.7 ± 2.5	18.8 ± 1.9	24.7 ± 2.5

LOI = loss on ignition.

### 3.2. X-ray Diffraction Characterisation

Figure 2 presents the X-ray powder diffraction patterns of raw end-of-life Lithuania cement–asbestos samples. Even though the samples were exposed to external weather conditions in varying degrees and times, the phase compositions for all tested samples were rather similar. On the X-ray diffraction patterns of all samples, diffraction reflexes from the cementitious matrix dominate. The main identified crystal components for all samples were calcite ( $\text{CaCO}_3$ ) and quartz ( $\text{SiO}_2$ ). As an asbestos mineral for all samples, chrysotile ( $\text{Mg}_3\text{Si}_2\text{O}_5(\text{OH})_4$ ) was detected, which was confirmed via the presence of the characteristic main reflex at  $\sim 12^\circ$  2Theta. Taking into account the MgO content from XRF tests, it can be estimated that the chrysotile content in the material is approximately 14 wt%. This is consistent with the typical asbestos content for cement–asbestos products. Besides the abovementioned phases, other mineral phases like aragonite ( $\text{CaCO}_3$ ), larnite ( $\text{Ca}_2\text{SiO}_4$ ), gypsum ( $\text{CaSO}_4 \cdot 2\text{H}_2\text{O}$ ), ettringite  $\text{Ca}_6\text{Al}_2(\text{SO}_4)_3(\text{OH})_{12} \cdot 26\text{H}_2\text{O}$  and brownmillerite ( $\text{Ca}_2(\text{Al}, \text{Fe})_2\text{O}_5$ ) were also identified. In the case of the V2 and V5 samples, a trace of portlandite ( $\text{Ca}(\text{OH})_2$ ) was also identified. Due to the long-time ageing and weathering of samples, some amorphous content was also confirmed.

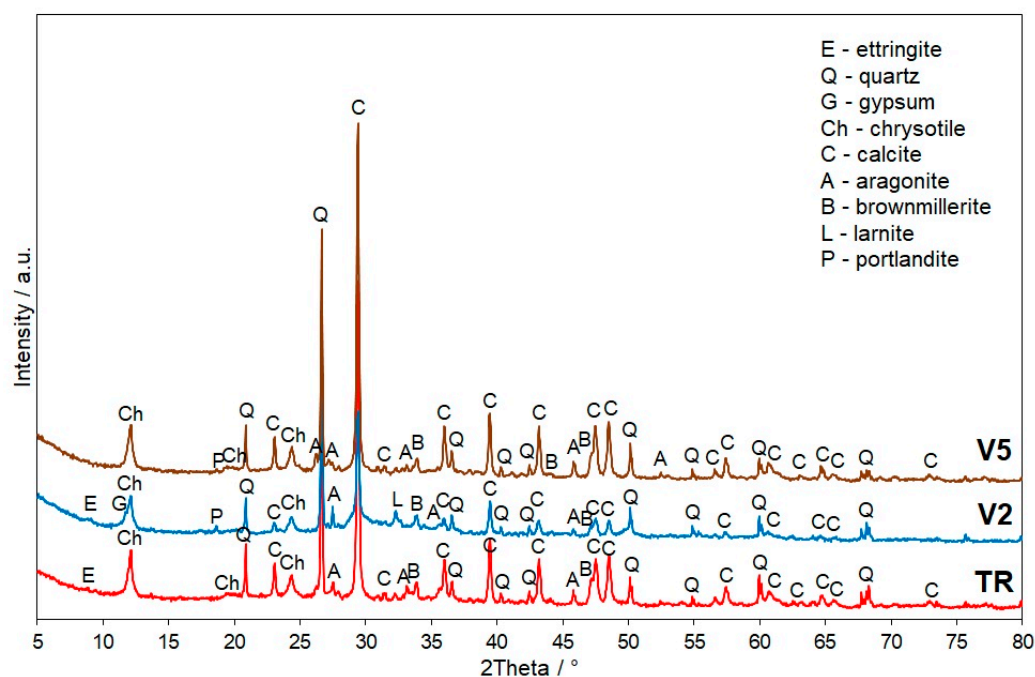


**Figure 2.** XRD patterns of end-of-life asbestos wastes.

### 3.3. Scanning Electron Microscopy Observation

SEM images of the considered cement–asbestos boards are presented in Figures 3 and 4. The surface for samples TR and V2 was rather smooth and compact, and bundles of asbestos fibres were well embedded in the cement matrix. In contrast to the previously mentioned sample, for V5, material bundles of asbestos fibres were poorly embedded in the matrix and were easily pulled out, which was related to the high degree of weathering of this type of cement–asbestos sample. The SEM image of this sample at a high magnification (Figure 4c) shows the presence of isolated, irregular grains of calcium carbonate. This was the main product of the 50-year ageing of the material.

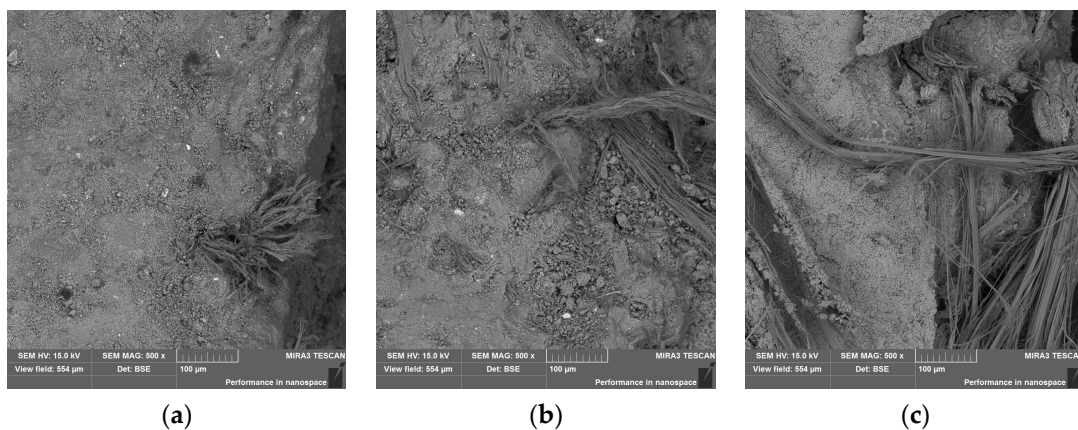


**Figure 3.** SEM images of raw end-of-life asbestos wastes: sample TR (a), V2 (b) and V5 (c); magn. 500 $\times$ .

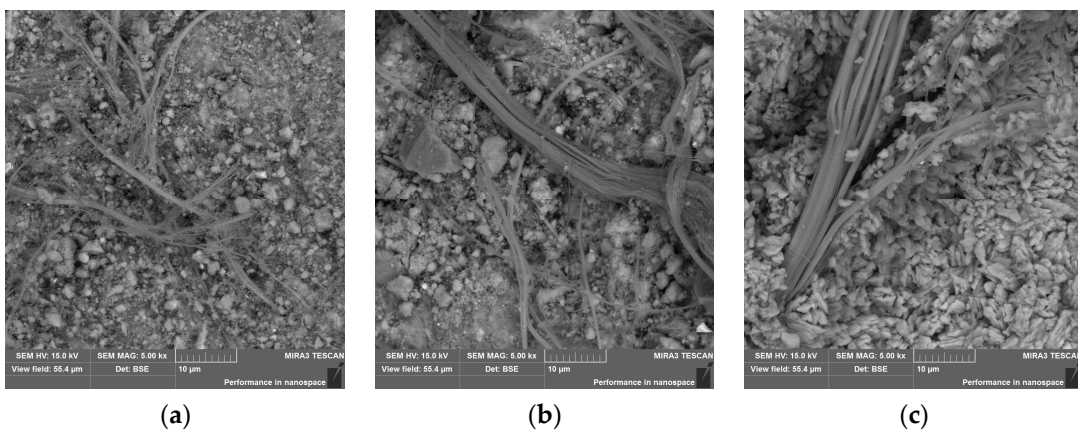


**Figure 4.** SEM images of raw end-of-life asbestos wastes: sample TR (a), V2 (b) and V5 (c); magn. 5000 $\times$ .

### 3.4. Thermal Analysis Characterisation

The qualitative progress of the thermal decomposition process of all tested cement–asbestos samples was generally very similar (Figure 5); however, for the V2 sample (Figure 5b), more varied behaviour was recorded. Comparing the main effects, changes in the intensity of individual effects were recorded, and can be related to the quantitative content of individual phases in each end-of-life cement–asbestos sample. In all obtained curves dominated effects connected to the decomposition of the cementitious matrix. Due to the relatively small amount of asbestos in cement–asbestos material and its overlap with another thermal effect at the same temperature range, no visible characteristic effects resulted from the thermal decomposition of pure chrysotile asbestos.

In the temperature range from 100 to 200 °C, on all DTA curves, the endothermic peak connected with mass change was observed. The  $T_{\max}$  value of this effect was changed from 144 °C for the TR sample to 163 °C in the case of the V5 sample. For all tested samples, this effect was a loss of water from the so-called CSH phase constituting the cementitious matrix. On DTG curves of all tested samples in this temperature range, the visible peak was identified, but their intensity changed significantly depending on the source of the sample. The lowest effect was registered in the case of the TR sample, while the strongest peak was observed in the case of the V2 sample. This sample was exposed to corrosion for the shortest period. Moreover, in the case of the V2 sample, on the DTG curve, a slight inflexion at around 200 °C is visible. This probably comes from the thermal decomposition of gypsum, which was identified via the XRD technique in this sample.

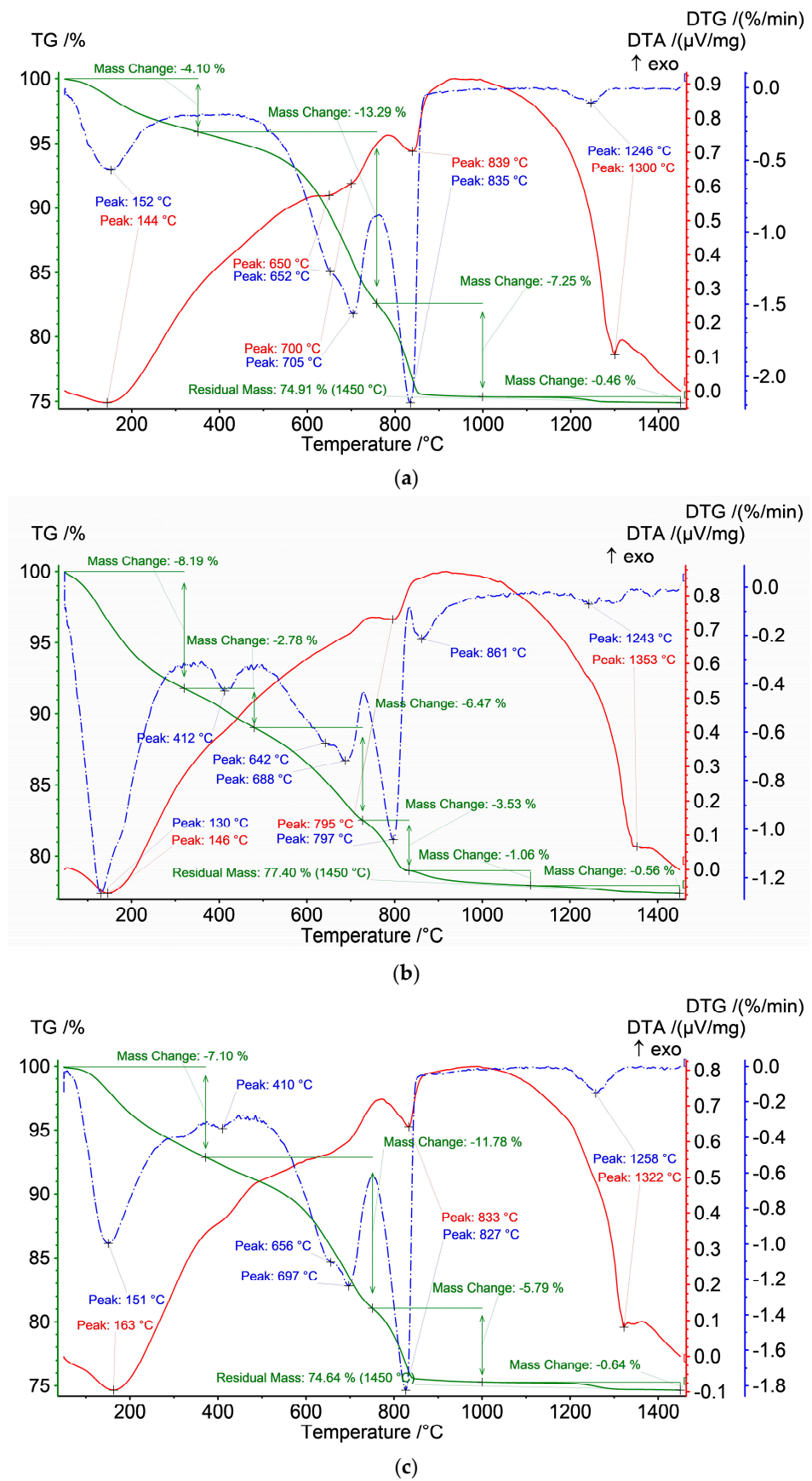
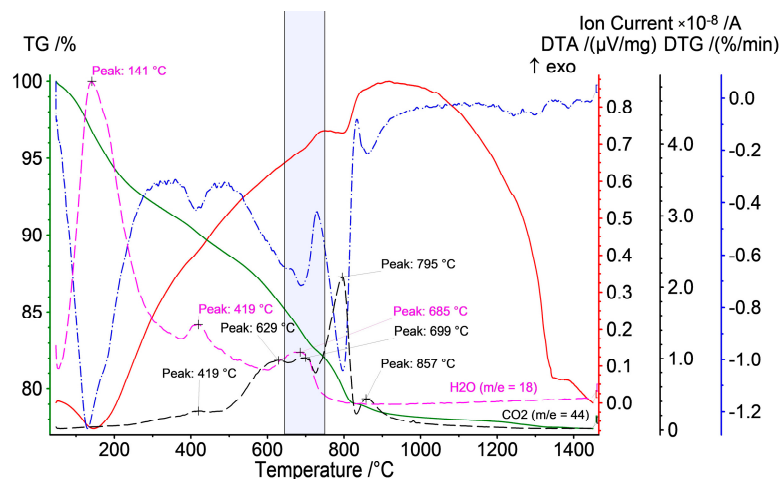


Figure 5. DTATG–DTG curves of tested asbestos wastes: sample TR (a), V2 (b) and V5 (c).

A very weak endothermic peak at  $\sim 410$  °C (visible mainly in the case of the V5 sample) indicates the presence of portlandite ( $\text{Ca}(\text{OH})_2$ ) and its thermal decomposition, which is more visible on the DTG curves of the V2 and V5 samples and in the presence of water in evolved gas (Figure 6). Contrary to another cement–asbestos sample described in the literature [54], the amount of  $\text{Ca}(\text{OH})_2$  is extremely little, and this phenomenon may be explained by the strong weathering of these samples.



**Figure 6.** Evolved gas analysis ( $\text{H}_2\text{O}$  and  $\text{CO}_2$ ) of the V2 sample with the area of chrysotile dehydroxylation marked.

At higher temperatures (in the range 600–850 °C), the decomposition of carbonates occurs, especially calcium carbonates ( $\text{CaCO}_3$ ; calcite and aragonite were identified in the samples). It can be noticed that this process takes place in two different stages. First, in the wide temperature range from 600 to 750 °C (the effect mainly is visible on DTA curves for the TR and V5 samples, i.e., samples with long-term ageing), it is connected with the release of water and part of the carbon dioxide from the samples. For the V2 sample, this effect is also identified but with a lower intensity (Figure 6). In this temperature range, the thermal decomposition of chrysotile asbestos should also take place; however, its characteristic thermal decomposition effects are masked by the decarbonisation of the cementitious matrix. On the other hand, on the water curve, in the temperature range corresponding to the decomposition of chrysotile, a small peak coming from  $\text{H}_2\text{O}$  evolution was observed (Figure 6, marked area), which may indicate the dehydroxylation process and thermal decomposition of chrysotile.

The second stage occurs at a higher temperature ( $\sim 800$  °C) and is visible as an endothermic effect on the DTA curves of all samples and a strong DTG peak mainly connected with the presence of carbon dioxide in the flue gas. Furthermore, in the case of the V2 sample, additional effect at  $\sim 860$  °C was observed, and it was connected with  $\sim 1$  wt% of weight loss. EGA analysis confirmed that, in this case, carbonate compounds also decompose thermally. A wide temperature range of  $\text{CO}_2$  release may indicate different degrees of crystallinity of calcium carbonates [55]. In the temperature range 1250–1350 °C on the TG curves of all tested cement–asbestos samples, small weight loss ( $\sim 0.5$ – $0.6$  wt%) was observed, and it indicated the presence of sulphur in the samples as a sulphate compound.

### 3.5. Characterisation of Materials after Thermal Treatment

The X-ray powder diffraction patterns of the materials obtained after the calcination at 1100 °C of raw end-of-life Lithuania cement–asbestos samples are presented in Figure 7. The phase compositions obtained for all tested samples were very similar and were dominated by diffraction reflexes coming from mineral phases like quartz ( $\text{SiO}_2$ ), akermanite ( $\text{Ca}_2\text{Mg}(\text{Si}_2\text{O}_7)$ ), larnite ( $\text{Ca}_2\text{SiO}_4$ ), monticellite ( $\text{Ca}(\text{Mg},\text{Fe})\text{SiO}_4$ ) and merwinite ( $\text{Ca}_3\text{Mg}(\text{SiO}_4)_2$ ). Moreover, in the case of the TR sample, additional reflexes coming from

forsterite ( $Mg_2SiO_4$ ) as well as magnetite ( $Fe_3O_4$ ) were also identified. Most of them were the result of the high-temperature synthesis of cement matrix ingredients with magnesium compounds from the product of chrysotile asbestos thermal decomposition. From a technological point of view, it is worth noting that, in all obtained diffraction patterns, no characteristic reflexes from asbestos minerals were recorded. This directly confirms that, in this thermal condition, asbestos decomposition occurred. Magnesium oxide released during the thermal decomposition of chrysotile was incorporated into the crystal structure of new minerals containing magnesium (like akermanite, monticellite, merwinite and forsterite), which were absent at the stage of characterisation of raw cement–asbestos wastes.

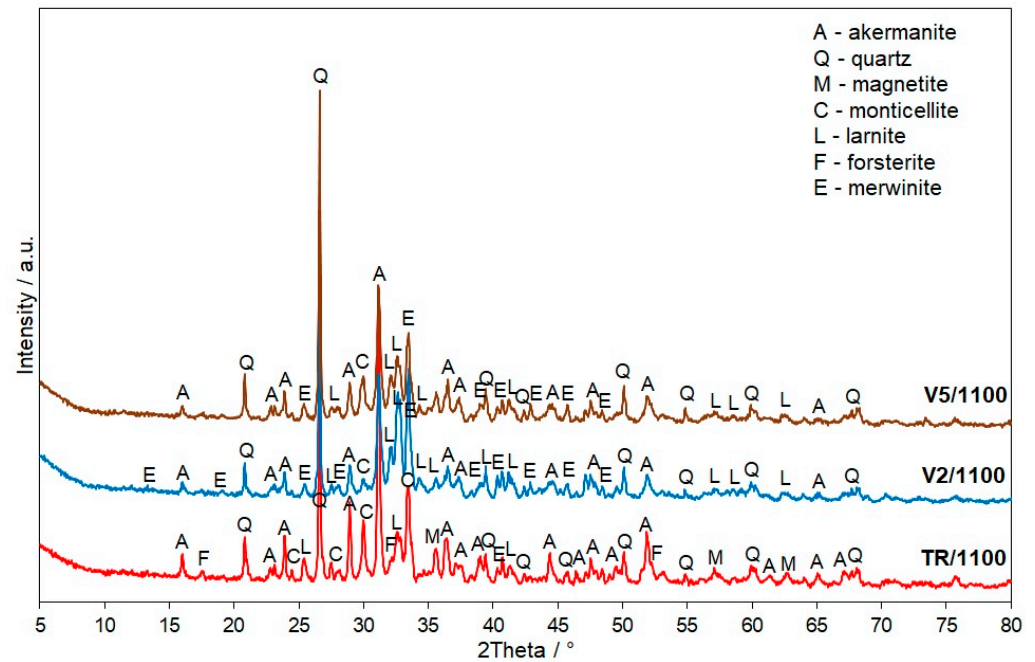


**Figure 7.** XRD patterns of cement–asbestos wastes after isothermal calcination at 1100 °C for 4 h.

SEM images of cement–asbestos samples after isothermal calcination are presented in Figure 8. The microphotographs show the samples after calcination at the specified temperature and manual grinding in an agate mortar. As can be observed, the material obtained was easy to grind and crush by hand, resulting in a fine powder without fibrous forms.

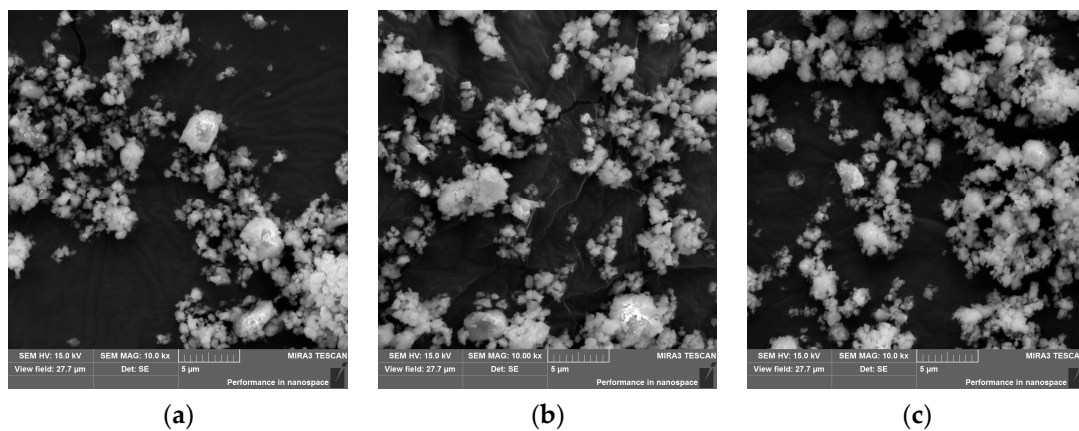


**Figure 8.** SEM images of asbestos wastes after thermal treatment: sample TR (a), V2 (b) and V5 (c); magn. 10,000×.

#### 4. Discussion

The obtained results of the chemical and phase compositions of three end-of-life cement-asbestos samples from Lithuania show that they are very similar materials. The course of thermal analysis (DTA/TG/DTG) curves and the characterisation of materials after isothermal calcination were also rather similar and indicated that the decomposition process similarly took place, without significant differences. The effect of the thermal processing of cement-asbestos wastes was to transform it into a material free of asbestos minerals. This is indicated by the phase compositions of the obtained materials.

Due to the fact that asbestos minerals belong to the group of hydrated silicates, they undergo an easy thermal decomposition process. As a result of the thermal processing of asbestos, chemically bound water is released, which in turn leads to a change in the crystal structure. As a consequence, the creation of new mineral phases occurs. At high temperatures, chrysotile converts into stable crystalline silicates through solid-state reactions [41–49,56,57]. In the temperature range from 650 to 750 °C, the dehydroxylation of chrysotile occurs and is followed by solid-state recrystallisation at a temperature exceeding 800 °C into forsterite ( $\text{Mg}_2\text{SiO}_4$ ) first and enstatite ( $\text{MgSiO}_3$ ) later via the following reaction:  $\text{Mg}_3(\text{OH})_4\text{Si}_2\text{O}_5 = \text{Mg}_2\text{SiO}_4 + \text{MgSiO}_3 + 2\text{H}_2\text{O}$ . During the reaction, chrysotile fibres preserved the same overall crystal habit, although a complete modification of the structure at the molecular scale occurred that is called the ‘pseudomorphosis phenomenon’ [51,58] (Figure 9). The removal of structural water (OH ions) from the crystal structure of asbestos causes an irreversible decrease in mechanical strength and next allows for the inclusion of Mg compounds in new mineral phases. The asbestos fibres lose their flexibility and can be easily transformed into powdered material, which was demonstrated by observing the crushed material after thermal treatment.

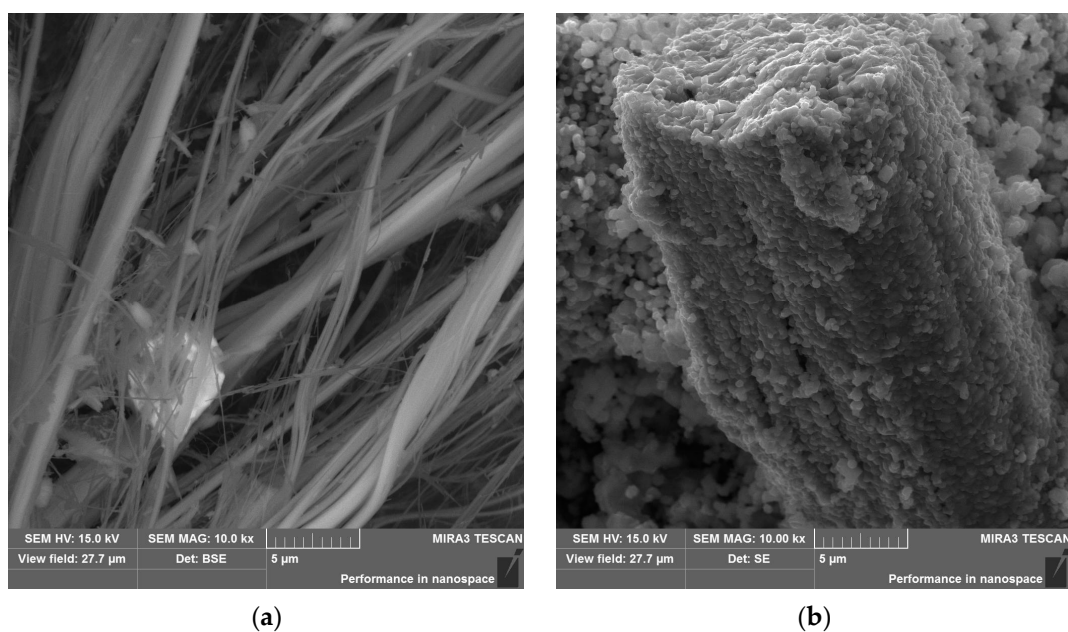


**Figure 9.** SEM images of raw asbestos bundle before (a) and after thermal treatment (b); magn. 10,000×.

More interesting conclusions can be drawn when the samples’ chemical and phase compositions are compared with those of other cement-asbestos wastes reported in the specialist literature [54,59–61]. When we compared the chemical composition of Lithuanian cement-asbestos end-of-life materials with that of another nine samples from Poland investigated previously by the authors [62], a significant difference in silica content was detected. This was visible in the chemical composition. For the tested Lithuanian samples, the content of  $\text{SiO}_2$  was approximately 33 wt% (Table 2), while during tests on Polish

cement–asbestos wastes, this content was much smaller and reached a level of ~20 wt%. This phenomenon was also observed under the phase analysis of raw waste samples. In the case of the tested Lithuanian samples, strong and visible powder diffraction reflexes of quartz were identified (Figure 2). This phenomenon was not found in the case of the Polish waste examined. This indicates a different technology for the production of cement–asbestos products in the past, where quartz sand was probably used as a mineral filler of the cementitious matrix.

In the broadest context, the variable chemical compositions may affect the material's behaviour at high temperatures. Due to the fact that cement–asbestos materials are composed mainly of CaO, SiO<sub>2</sub> and MgO, the triangular diagram of these oxides should be considered and chosen for analysis. Knowing the chemical composition of all tested samples, we can plot composition points on the diagram (Figure 10). As can be observed, Lithuanian end-of-life asbestos wastes (marked as V2, V5 and TR) constitutes a separate group of wastes in terms of possible thermal treatment. Their chemical composition points distinctly lie in the area of increased SiO<sub>2</sub> content compared with that of Polish waste (points from 1 to 10) and simultaneously in other stability fields of phases in the equilibrium state. Lithuanian samples crossed the stability fields of pseudo-wollastonite (CaSiO<sub>3</sub>) and akermanite (Ca<sub>2</sub>MgSi<sub>2</sub>O<sub>7</sub>), while for the Polish sample, they gathered in the surrounding areas of the contact stability fields of lime (CaO), periclase (MgO) and belite (Ca<sub>2</sub>SiO<sub>4</sub>).

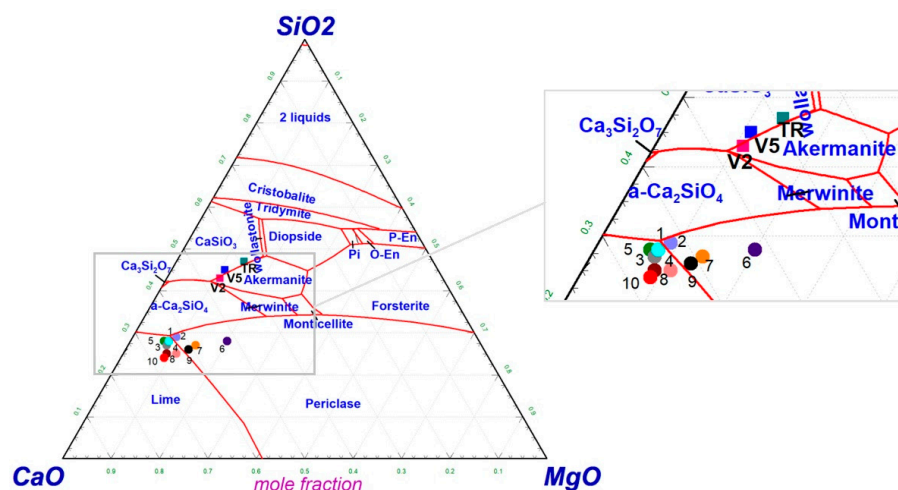


**Figure 10.** Points corresponding to samples (TR, V2 and V5) under study in the CaO–MgO–SiO<sub>2</sub> system in comparison with previously studied cement–asbestos materials (1–10 dots).

Our findings are consistent with the observations and research presented by Viani et al. [54,60], who also demonstrated the variable compositions of cement–asbestos samples. Three classes with different C/S ratios and dominant mineralogy were reported by the authors. The studied Lithuanian samples were close to a group of samples, the corresponding points lay inside the stability field of akermanite. The other samples studied (by Viani et al.) were samples that fell into the stability field of merwinite or samples that lie on the boundary between the stability field of belite (Ca<sub>2</sub>SiO<sub>4</sub>) and that of periclase. Moreover, it can be concluded that Polish samples can create a new class of cement–asbestos wastes with high lime (CaO) content. These differences may contribute to the formation of different mineral phases during thermal treatment in the context of the formation of mineral binder components [63]. The secondary use of waste processed in this way is possible in the production of various building materials (for example, an additive for cement) via the design of their composition and taking into account the chemical composition of the additive and its stability.

## 5. Conclusions

For the first time, we investigated the thermal decomposition process of cement–asbestos wastes from Lithuania. Thermal treatment is one of the possible methods for end-of-life asbestos-containing materials including also cement–asbestos products. There are no significant differences between the thermal decompositions of tested cement–asbestos samples from Lithuania. In each case, the thermal decomposition route took place similarly. As a result of this process, the asbestos minerals were changed by the solid-state reaction, and the final product of thermal treatment did not contain asbestos minerals. This product can be regarded as a potential secondary raw material in various industries; however, this requires an expansion of the scope of research to include medical tests demonstrating the harmlessness of the obtained material.

Moreover, when we compare these obtained results with those of samples from another country, it can be concluded that different production methods were applied for cement–asbestos production. This was mainly manifested by the increased silica content in the material, which in turn affected the formation of the final phase composition after thermal treatment. This should be kept in mind when considering possible recycling methods and the reuse of the resulting secondary raw material.

**Author Contributions:** Conceptualisation, R.K. and V.A.; methodology, R.K., V.A. and R.B.; validation, R.K., V.A., A.G., M.K. and R.B.; formal analysis, R.K. and V.A.; investigation, R.K., A.G. and R.B.; resources, R.K. and V.A.; data curation, R.K., V.A., R.B., A.G. and M.K.; writing—original draft preparation, R.K. and M.K.; writing—review and editing, R.K., V.A., R.B., A.G. and M.K.; visualisation, R.K., A.G. and M.K.; supervision, R.K. and V.A.; project administration, R.K.; funding acquisition, R.K. All authors have read and agreed to the published version of the manuscript.

**Funding:** This research was funded in whole by the National Science Centre, Poland, under “Sonata 17”, grant number UMO-2021/43/D/ST5/00356. For Open Access, the author has applied a CC-BY public copyright licence to any author-accepted manuscript (AAM) version arising from this submission.

**Data Availability Statement:** The original data presented in the study are openly available in RepOD repository <https://doi.org/10.18150/XCDVXX> (accessed on 16 January 2024).

**Acknowledgments:** The authors would like to thank Elwira Cieślińska and Maria Pyka for their help in preparing samples for testing.

**Conflicts of Interest:** The authors declare no conflicts of interest.

## References

1. Virta, R.L. *Mineral Commodity Profiles—Asbestos*; Circular 1255-KK; U.S. Geological Survey: Reston, VA, USA, 2005.
2. Ciullo, P.A. *Industrial Minerals and Their Uses—A Handbook and Formulary*, 1st ed.; William Andrew Publishing: New York, NY, USA, 1996.
3. Gualtieri, A.F. *Mineral Fibres: Crystal Chemistry, Chemical-Physical Properties, Biological Interaction and Toxicity*; European Mineralogical Union: London, UK, 2017.
4. Sporn, T.A. Mineralogy of asbestos. In *Malignant Mesothelioma*; Tannapfel, A., Ed.; Springer: Berlin/Heidelberg, Germany, 2011; pp. 1–11.
5. Howe-Grant, M. *Kirk-Othmer Encyclopedia of Chemical Technology*, 4th ed.; John Wiley & Sons: Hoboken, NJ, USA, 1997.
6. Wallis, S.L.; Emmett, E.A.; Hardy, R.; Casper, B.B.; Blanchon, D.J.; Testa, J.R.; Menges, C.W.; Gonneau, C.; Jerolmack, D.J.; Seiphoori, A.; et al. Challenging global waste management—Bioremediation to detoxify asbestos. *Front. Environ. Sci.* **2020**, *8*, 20. [[CrossRef](#)] [[PubMed](#)]
7. Huang, S.X.L.; Jaurand, M.-C.; Kamp, D.W.; Whysner, J.; Hei, T.K. Role of mutagenicity in asbestos fiber-induced carcinogenicity and other diseases. *J. Toxicol. Environ. Health B Crit. Rev.* **2011**, *1–4*, 179–245. [[CrossRef](#)] [[PubMed](#)]
8. Cheng, T.J.; More, S.L.; Maddaloni, M.A.; Fung, E.S. Evaluation of potential gastrointestinal carcinogenicity associated with the ingestion of asbestos. *Rev. Environ. Health* **2021**, *26*, 15–26. [[CrossRef](#)] [[PubMed](#)]
9. Kwak, K.; Kang, D.; Paek, D. Environmental exposure to asbestos and the risk of lung cancer: A systematic review and meta-analysis. *J. Occup. Environ. Med.* **2022**, *79*, 207–214. [[CrossRef](#)] [[PubMed](#)]
10. Musk, A.W.; de Klerk, N.; Reid, A.; Hui, J.; Franklin, P.; Brims, F. Asbestos-related diseases. *Int. J. Tuberc. Lung Dis.* **2020**, *24*, 562–567. [[CrossRef](#)] [[PubMed](#)]

11. Stayner, L.; Welch, L.S.; Lemen, R. The worldwide pandemic asbestos-related diseases. *Annu. Rev. Public Health* **2013**, *34*, 205–216. [[CrossRef](#)] [[PubMed](#)]
12. Lin, R.T.; Chien, L.C.; Jimba, M.; Furuya, S.; Takahashi, K. Implementation of national policies for a total asbestos ban: A global comparison. *Lancet Planet Health* **2019**, *3*, 341–348. [[CrossRef](#)]
13. The International Ban Asbestos Secretariat IBAS. Available online: [www.ibasecretariat.org/index.htm](http://www.ibasecretariat.org/index.htm) (accessed on 18 December 2023).
14. Ulewicz, M. Management of asbestos materials in terms of life and work safety. *Przegląd Bud.* **2023**, *9/10*, 171–176. (In Polish) [[CrossRef](#)]
15. Flanagan, D.M. *Mineral Commodity Summaries. Asbestos 2022*; U.S. Geological Survey: Reston, VA, USA, 2023.
16. European Commission. *European Commission Directive 1999/77/EC, 26 July 1999*; European Commission: Brussels, Belgium, 1999. Available online: <https://eur-lex.europa.eu/eli/dir/1999/77/oj> (accessed on 13 December 2023).
17. Sejm of the Republic of Poland. *Act on the Prohibition of the Use of Asbestos-Containing Products, 19 June 1997*; Sejm of the Republic of Poland: Warsaw, Poland, 1997. Available online: <https://isap.sejm.gov.pl/isap.nsf/DocDetails.xsp?id=WDU19971010628> (accessed on 13 December 2023). (In Polish)
18. Council of Ministers of the Republic of Poland. *Program for the Removal of Asbestos and Asbestos-Containing Products Used in Poland*; Polish Government: Warsaw, Poland, 2002.
19. Smolianskiene, G.; Adamoniene, D.; Šeškauskas, V. Studies on occupational asbestos in Lithuania: Achievements and problems. *Indoor Built Environ.* **2005**, *14*, 331–335. [[CrossRef](#)]
20. Smailyte, G.; Kurtinaitis, J.; Andersen, A. Cancer mortality and morbidity among Lithuanian asbestos-cement producing workers. *Scand. J. Work Environ. Health* **2004**, *30*, 64–70. [[CrossRef](#)]
21. Smailyte, G.; Kurtinaitis, J.; Andersen, A. Mortality and cancer incidence among Lithuanian cement producing workers. *Occup. Environ. Med.* **2004**, *61*, 529–534. [[CrossRef](#)] [[PubMed](#)]
22. Kanarek, M.S. Mesothelioma from chrysotile asbestos: Update. *Ann. Epidemiol.* **2011**, *21*, 688–697. [[CrossRef](#)] [[PubMed](#)]
23. European Commission. *European Commission Directive 80/1107/EEC, 27 November 1980*; European Commission: Brussels, Belgium, 1980. Available online: <https://eur-lex.europa.eu/legal-content/EN/ALL/?uri=CELEX:31980L1107> (accessed on 13 December 2023).
24. European Commission. *European Commission Directive 83/477/EEC, 19 September 1983*; European Commission: Brussels, Belgium, 1983. Available online: <https://eur-lex.europa.eu/legal-content/EN/TXT/?uri=CELEX:31983L0477> (accessed on 13 December 2023).
25. European Commission. *European Commission Directive 91/382/EEC, 25 June 1991*; European Commission: Brussels, Belgium, 1991. Available online: <https://eur-lex.europa.eu/legal-content/EN/TXT/?uri=CELEX:31991L0382> (accessed on 13 December 2023).
26. Petrauskait Everatt, R.; Smolianskiene, G.; Tossavainen, A.; Cicėnas, S.; Jankauskas, R. Occupational characteristics of respiratory cancer patients exposed to asbestos in Lithuania. *J. Phys. Conf. Ser.* **2009**, *151*, 012012. [[CrossRef](#)]
27. Kusiorowski, R.; Lipowska, B.; Kujawa, M.; Gerle, A. Problem of asbestos-containing wastes in Poland. *Clean. Waste Syst.* **2023**, *4*, 100085. [[CrossRef](#)]
28. Brzana, W.; Buczaj, A.; Nowak, J.; Nowak, D. Concentrations of asbestos fibres at wild asbestos wastes dumping grounds. *Med. Og. Nauk Zdr.* **2014**, *20*, 98–101. (In Polish)
29. Opinion of the European Economic and Social Committee on ‘An EU without Asbestos’; OJ C 251, 31.7.2015. Available online: <https://eur-lex.europa.eu/legal-content/EN/TXT/?uri=CELEX:52014IE5005&qid=1712828554838> (accessed on 13 December 2023).
30. EU Parliament, Document 52020DC0098, A New Circular Economy Action Plan for a Cleaner and More Competitive Europe. Available online: <https://eur-lex.europa.eu/legal-content/EN/TXT/?uri=COM:2020:98:FIN> (accessed on 18 December 2023).
31. Gualtieri, A.F. Recycling asbestos-containing material (ACM) from construction and demolition waste (CDW). In *Handbook of Recycled Concrete and Demolition Waste*; Pacheco-Torgal, F., Tam, V.W.Y., Labrincha, J.A., Ding, Y., de Brito, J., Eds.; Woodhead Publishing: Cambridge, UK, 2013; Volume 47, pp. 500–525.
32. Spasiano, D.; Pirozzi, F. Treatments of asbestos-containing wastes. *J. Environ. Manag.* **2017**, *204*, 82–91. [[CrossRef](#)] [[PubMed](#)]
33. Paolini, V.; Tomassetti, L.; Segreto, M.; Borin, D.; Liotta, F.; Torre, M.; Petracchini, F. Asbestos treatment technologies. *J. Mater. Cycles Waste Manag.* **2019**, *21*, 205–226. [[CrossRef](#)]
34. Lim, Y.; Jang, H.; So, S. Evaluation of mineral carbonation of asbestos-tex and analysis of airborne asbestos concentrations. *Buildings* **2022**, *12*, 1372. [[CrossRef](#)]
35. Trapasso, F.; Croci, D.; Plescia, P.; Tempesta, E. Asbestos waste carbonation: A new asbestos treatment with CO<sub>2</sub> recovery. In *Proceedings of the 3rd International Conference on Industrial and Hazardous Waste Management, Chania, Greece, 12–14 September 2012*; pp. 1–8.
36. Oskierski, H.C.; Długogorski, B.Z.; Jacobsen, G. Sequestration of atmospheric CO<sub>2</sub> in chrysotile mine tailings of the Woodsreef Asbestos Mine, Australia: Quantitative mineralogy, isotopic fingerprinting and carbonation rates. *Chem. Geol.* **2013**, *358*, 156–169. [[CrossRef](#)]
37. Saran, R.K.; Arora, V.; Yadav, S. CO<sub>2</sub> sequestration by mineral carbonation: A review. *Glob. NEST J.* **2018**, *20*, 497–503.
38. Brycht, N. Recycling of asbestos-cement waste—An opportunity or a threat? *CzOTO* **2022**, *4*, 10–18. [[CrossRef](#)]

39. Sobik-Szołtysek, J. Asbestos waste in Poland—The present state and perspectives of management. In *Inżynieria Środowiska I Biotechnologia. Wyzwania i Nowe Technologie*; Rosińska, A., Karwowska, B., Madeła, M., Eds.; Wydawnictwo Politechniki Częstochowskiej: Częstochowa, Poland, 2023; pp. 294–318. (In Polish)
40. Obmiński, A. Asbestos waste recycling using the microwave technique—Benefits and risks. *Environ. Nanotechnol. Monit. Manag.* **2021**, *16*, 100577. [[CrossRef](#)]
41. Bloise, A.; Kusiorowski, R.; Lassinantti Gualtieri, M.; Gualtieri, A.F. Thermal behaviour of mineral fibres. In *Mineral Fibres: Crystal Chemistry, Chemical-Physical Properties, Biological Interaction and Toxicity*; Gualtieri, A.F., Ed.; European Mineralogical Union: London, UK, 2017; pp. 215–260.
42. Kusiorowski, R.; Zaremba, T.; Piotrowski, J.; Adamek, J. Thermal decomposition of different types of asbestos. *J. Therm. Anal. Calorim.* **2012**, *109*, 693–704. [[CrossRef](#)]
43. Zaremba, T.; Krzakała, A.; Piotrowski, J.; Garczorz, D. Study on the thermal decomposition of chrysotile asbestos. *J. Therm. Anal. Calorim.* **2010**, *101*, 479–485. [[CrossRef](#)]
44. Cattaneo, A.; Gualtieri, A.F.; Artioli, G. Kinetic study of the dehydroxylation of chrysotile asbestos with temperature by in situ XRPD. *Phys. Chem. Miner.* **2003**, *30*, 177–183. [[CrossRef](#)]
45. Gualtieri, A.F.; Levy, D.; Belluso, E.; Dapiaggi, M. Kinetics of the decomposition of crocidolite asbestos: A preliminary real-time X-ray powder diffraction study. *Mater. Sci. Forum* **2004**, *443–444*, 291–294. [[CrossRef](#)]
46. Gualtieri, A.F.; Giacobbe, C.; Sardisco, L.; Saraceno, M.; Gualtieri, M.L.; Lusvardi, G.; Cavenati, C.; Zanatto, I. Recycling of the product of thermal inertization of cement-asbestos for various industrial applications. *Waste Manag.* **2011**, *31*, 91–100. [[CrossRef](#)]
47. Gualtieri, A.F.; Tartaglia, A. Thermal decomposition of asbestos and recycling in traditional ceramics. *J. Europ. Ceram. Soc.* **2000**, *20*, 1409–1418. [[CrossRef](#)]
48. Gualtieri, A.F.; Cavenati, C.; Zanatto, I.; Meloni, M.; Elmi, G.; Gualtieri, M.L. The transformation sequence of cement-asbestos slates up to 1200 °C and safe recycling of the reaction product in stoneware tile mixtures. *J. Hazard. Mater.* **2008**, *152*, 563–570. [[CrossRef](#)]
49. Kusiorowski, R.; Zaremba, T.; Piotrowski, J.; Gerle, A. Thermal decomposition of asbestos-containing materials. *J. Therm. Anal. Calorim.* **2013**, *113*, 179–188. [[CrossRef](#)]
50. Kusiorowski, R.; Zaremba, T.; Piotrowski, J.; Podwórny, J. Utilisation of cement-asbestos wastes by thermal treatment and the potential possibility use of obtained product for the clinker bricks manufacture. *J. Mater. Sci.* **2015**, *50*, 6757–6767. [[CrossRef](#)]
51. Kusiorowski, R.; Lipowska, B.; Gerle, A. Synthesis of ye’elimite from anthropogenic waste. *Minerals* **2023**, *13*, 137. [[CrossRef](#)]
52. Vergani, F.; Galimberti, L.; Marian, N.M.; Giorgetti, G.; Viti, C.; Capitani, G. Thermal decomposition of cement-asbestos at 1100 °C: How much “safe” is “safe”? *J. Mater. Cycles Waste Manag.* **2022**, *24*, 297–310. [[CrossRef](#)]
53. *EN ISO 12677:2011*; Chemical Analysis of Refractory Products by X-ray Fluorescence (XRF)—Fused Cast-Bead Method. ISO: Geneva, Switzerland, 2011.
54. Viani, A.; Gualtieri, A.F.; Secco, M.; Peruzzo, L.; Artioli, G.; Cruciani, G. Crystal chemistry of cement-asbestos. *Am. Mineral.* **2013**, *98*, 1095–1105. [[CrossRef](#)]
55. Dias, C.M.R.; Cincotto, M.A.; Savastano, H., Jr.; John, V.M. Long-term aging of fiber-cement corrugated sheets—The effect of carbonation, leaching and acid rain. *Cem. Concr. Compos.* **2008**, *30*, 255–265. [[CrossRef](#)]
56. Martin, C.J. The thermal decomposition of chrysotile. *Mineral. Mag.* **1977**, *35*, 189–195. [[CrossRef](#)]
57. MacKenzie, K.J.D.; Meinhold, R.H. Thermal reactions of chrysotile revisited: A <sup>29</sup>Si and <sup>25</sup>Mg MAS NMR study. *Am. Mineral.* **1994**, *79*, 43–50.
58. Giacobbe, C.; Gualtieri, A.F.; Quartieri, S.; Rinaudo, C.; Allegrina, M.; Andreozzi, G.B. Spectroscopic study of the product of thermal transformation of chrysotile-asbestos containing materials (ACM). *Eur. J. Mineral.* **2010**, *22*, 535–546. [[CrossRef](#)]
59. Belardi, C.; Piga, L. Influence of calcium carbonate on the decomposition of asbestos contained in end-of-life products. *Thermochim. Acta* **2013**, *573*, 220–228. [[CrossRef](#)]
60. Viani, A.; Gualtieri, A.F.; Pollastri, S.; Rinaudo, C.; Croce, A.; Urso, G. Crystal chemistry of the high temperature product of transformation of cement-asbestos. *J. Hazard. Mater.* **2013**, *248–249*, 69–80. [[CrossRef](#)]
61. Witek, J.; Kusiorowski, R. Neutralization of cement-asbestos waste by melting in an arc-resistance furnace. *Waste Manag.* **2017**, *69*, 336–345. [[CrossRef](#)] [[PubMed](#)]
62. Kusiorowski, R.; Gerle, A.; Kujawa, M.; Śliwa, A.; Adamek, J. Characterisation of asbestos-containing wastes by thermal analysis. *J. Therm. Anal. Calorim.* **2024**, submitted.
63. Scrivener, K.; Nonat, A. Hydration of cementitious materials, present and future. *Cem. Concr. Res.* **2011**, *41*, 651–665. [[CrossRef](#)]

**Disclaimer/Publisher’s Note:** The statements, opinions and data contained in all publications are solely those of the individual author(s) and contributor(s) and not of MDPI and/or the editor(s). MDPI and/or the editor(s) disclaim responsibility for any injury to people or property resulting from any ideas, methods, instructions or products referred to in the content.